

## Intersystem Crossings in Model Energetic Materials

M. Riad Manaa\* and Laurence E. Fried

University of California, Lawrence Livermore National Laboratory, Chemistry and Materials Science Directorate, P.O. Box 808, L-282, Livermore, California 94551

Received: July 19, 1999; In Final Form: September 23, 1999

We consider the role of the lowest singlet–triplet intersystem crossing in molecular nitromethane, nitramine, and nitric acid using *ab initio* complete active space self-consistent field (CAS SCF) wave functions. These systems represent the simplest models of C–(NO<sub>2</sub>), N–(NO<sub>2</sub>), and O–(NO<sub>2</sub>) bonds in energetic materials. The lowest triplet state of these molecules exhibits a minimum equilibrium structure where the nitro group is no longer coplanar with the X (C, N, O) atom, in contrast to the equilibrium geometry of the ground-state singlets. CAS SCF and density functional theory (DFT) fully optimized triplet potential energy curves confirm that the triplets are adiabatically bound with respect to X–(NO<sub>2</sub>) bond dissociation pathway, with energy barriers at the CAS SCF level of 33, 25, and 15 kcal/mol, respectively. DFT optimizations produced barriers 9–15 kcal/mol lower than the CAS SCF. Singlet–triplet minimum energy crossing points have been located at 13, 8, and 4 kcal/mol above the respective triplet minima. The reported calculations should predict fast nonradiative transitions due to the crossings with the ground surfaces. This prediction is discussed in connection with the energetic properties of these systems.

### I. Introduction

Intersystem crossings are important in the energy deactivation processes of excited states. In cases where the intersystem crossing involves the first excited singlet and lowest triplet states of the molecular system, it is a key for the determination of the excited-state lifetime and the triplet-state formation, which are fundamental quantities in understanding the dynamics of many photophysical and photochemical processes.<sup>1</sup> Since the crossing of two  $N$  dimensional singlet and triplet potential energy surfaces occurs on the  $N - 1$  dimensional hypersurface, particularly relevant is the location of the lowest-energy point on the crossing surface. It is in the vicinity of this point, termed the minimum-energy crossing point (MECP), that transitions between the two states occur. From a computational *ab initio* perspective, recent advances in analytic gradient based techniques allow *direct* determination of this point,<sup>2</sup> including multireference and configuration interaction correlated methods.<sup>3–5</sup>

Many energetic materials consist of organic molecules containing the nitro group (NO<sub>2</sub>).<sup>6</sup> This group is most commonly bonded with carbon, nitrogen, or oxygen. The simplest representatives of such compounds are nitromethane for the C–(NO<sub>2</sub>) bond, nitramine for the N–(NO<sub>2</sub>) bond, and nitric acid for the O–(NO<sub>2</sub>) bond. Upon initiation with an external stimulus, energetic materials undergo rapid chemical transformation producing such typical gases as CO<sub>2</sub>, CO, N<sub>2</sub>, and H<sub>2</sub>O. Little is known about reaction mechanisms leading to these products.<sup>7</sup> For the simple case of nitromethane (CH<sub>3</sub>NO<sub>2</sub>), for example, recent experimental studies have suggested bimolecular,<sup>8,9</sup> C–N bond cleavage,<sup>10</sup> or ionic<sup>11</sup> decomposition mechanisms to be operative under various pressure regimes. Furthermore, the role of energy redistribution resulting from the exothermic chemical reactions involved in the decomposition process is still largely unclear. This is particularly important under shock conditions, since the energy release drives and sustains the shock wave front.

Different mechanisms have been proposed relating to the initial effect of mechanical energy transfer from a shock front to energetic molecules. The vibrational energy up-pumping model<sup>12</sup> suggests that the shock wave produces a bath of excited phonons absorbed by the lowest vibrational modes of molecules that make up the crystal. Increased phonon absorption and intramolecular vibrational energy redistribution (IVR) lead to excitation of higher frequency modes, eventually leading to an equilibrium transition state, chemical bond breakage, and subsequent chemical reactions.<sup>13</sup> The rate of phonon-to-vibron energy transfer has been related to the sensitivity in common explosives.<sup>14</sup> Williams,<sup>15</sup> on the other hand, was the first to consider the influence of electronic states and electronic transport on the initiation and propagation of detonation waves in solid explosives. Dremin et al.,<sup>16</sup> noting evidence for similarities between shock decomposition intermediates and those of photochemical processes, proposed electronic excitation as the first molecular response in their multiprocess detonation model. Furthermore, correlation of impact sensitivity with electronic levels of a homologous series of explosive compounds has been reported.<sup>17</sup> Finally, Gilman<sup>18</sup> proposed that the compression from the wave front causes local metallization when bending of covalent bonds, for instance, decreases the HOMO–LUMO gap.

In this work, we consider the role of the lowest singlet–triplet intersystem crossing in the simplest model energetic materials: molecular nitromethane, nitramine, and nitric acid. These are simple analogues of commonly used energetic materials such as TATB (1,3,5-triamino-2,4,6-trinitrobenzene), RDX (hexahydro-1,3,5-trinitro-*s*-triazine), and PETN (2,2-bis-[(nitrooxy)methyl]-1,3-propanediol dinitrate). We report, on the basis of *ab initio* CAS SCF calculations, minimum-energy crossing points between the lowest triplet state and the ground-state singlet located at 13, 8, and 4 kcal/mol above the respective triplet minima. The location of these crossings, near the triplet equilibrium minima, is unexpected, since they are more com-

\* To whom correspondence should be addressed. E-mail: manaa1@llnl.gov, lfried@llnl.gov.

monly encountered when molecular bonds are significantly stretched. Their existence should establish a nonradiative transition mechanism to deactivate the excited state population, leading to fast molecular decomposition on the ground-state surface. Moreover, we show that the triplet states are adiabatically bound with respect to the X-NO<sub>2</sub> bond dissociation pathway. The reported results should provide further insight into the gas-phase photochemistry of these important compounds and into initiation models involving excited electronic states of energetic materials.

## II. Computational Methods

The reported calculations were performed using two basis sets. Dunning's double- $\zeta$  plus polarization (dzp) basis<sup>19</sup> was used in the CAS SCF singlet-triplet minimum energy crossing search and the equilibrium structure optimizations. The larger 6-311++G(2d,2p) (C, N, O, 5s4p2d; H, 4s2p) basis was used in CAS SCF and DFT potential energy curves optimization and single-point calculations.

The active space in the CAS SCF calculations<sup>20,21</sup> was based on six electrons distributed in five orbitals. In the ground-state geometry, two orbitals represent the  $\sigma$  and  $\sigma^*$  of the C-N, N-N, and O-N bonds. Of the remaining three, one is a nonbonding and two are the  $\pi$  and  $\pi^*$  of the NO<sub>2</sub> group. This treatment, referred to as CAS(6,5) hereafter, describes the three molecular systems' singlet and triplet states, which form degenerate pairs at the corresponding dissociation limit. In addition, a larger active space consisting of eight electrons in eight orbitals, CAS (8,8), was used in the equilibrium optimization of the singlet and triplet states of nitromethane. The extra two orbitals represent the  $\sigma$  and  $\sigma^*$  of C-H.

In our ongoing effort to monitor the performance of DFT methods for both closed and open-shell systems, we chose the hybrid B3LYP functional in the DFT calculations. B3LYP refers to Becke's three-parameter exchange functional<sup>22</sup> along with the nonlocal correlation functional of Lee, Yang, and Parr.<sup>23</sup> This functional was selected, since it provided the best results on an open-shell system as reported in our previous study.<sup>24</sup>

The CAS SCF minimum energy crossing search<sup>5</sup> is based on a state-averaged procedure, with the singlet and triplet states having equal weights (0.5). These calculations, along with the DFT optimizations, are part of the Gaussian 94 package of codes,<sup>25</sup> which was used with its default convergence criteria for the energies and wave functions. The multiconfiguration (MC) SCF method in the GAMESS program<sup>26</sup> was used for full curve optimizations using the active spaces and basis sets noted above. Single-point calculations using this program do not use state averaging, and the energetics at key points are comparable with the state-averaged results.

All calculations were performed without any symmetry constraint. For curve optimization, the C-(NO<sub>2</sub>), N-(NO<sub>2</sub>), and O-(NO<sub>2</sub>) bond distances were fixed at a given value while the rest of the molecular parameters were optimized. The triplet potential energy curves were calculated in the range  $R(X-NO_2) = 1.3-4.0$  Å.

## III. Results and Discussion

**1. Equilibrium Structures and Dissociation Curves.** The optimized singlet- and triplet-state equilibrium geometries and the singlet-triplet minimum energy crossing points are reported in Tables 1-3 for the three molecular species at various levels of theory. For nitromethane, we recently reported in a comparative study<sup>24</sup> the fully optimized curves with respect to C-N dissociation of both singlet and triplet states using DFT, CAS

**TABLE 1: Equilibrium Structures and Total Energies (in hartree) for the Singlet Ground State, the Triplet State, and the Singlet-Triplet Intersection of Nitromethane<sup>a</sup>**

	singlet <sup>b</sup>	triplet <sup>c</sup>	singlet-triplet MECP
$R(C-H_1)$	1.081 (1.086) 1.081	1.084 1.084 1.081	1.084
$R(C-H_{2,3})$	1.078 (1.082) 1.078	1.080 1.080 1.077	1.082
$R(C-N)$	1.476 (1.493) 1.473	1.460 (1.464) 1.459 1.489	1.460
$R(N-O)$	1.223 (1.229) 1.241	1.325 (1.305) 1.348 1.336	1.374
$\angle H_2CH_1$	110.2 110.2	110.0 110.1 110.4	110.4
$\angle NCH_1$	107.5 (106.78) 107.5	111.0 111.0 110.5	111.4
$\angle NCH_{2,3}$	108.0 (107.92) 108.0	107.8 107.8 107.4	107.8
$\angle CNO$	117.4 (117.09) 117.7	114.8 (118.5) 115.1 114.6	111.0
$\angle ONO$	124.6 124.7	111.1 110.2 111.2	94.3
$\angle ONOC$	178.4 178.4	132.9 132.3 132.3	113.6
$E_e$	-243.813 205 -243.878 779	-243.716 309 -243.777 799 -243.780 868	-243.694 444
ZPE	33.2	31.2	

<sup>a</sup> Results (top to bottom) are from CAS(6,5)/dzp, CAS(8,8)/dzp, and CAS SCF (8,8)/6-311++G(2d,2p) levels of theory, respectively. Bond lengths are in angstroms, and angles are in degrees. <sup>b</sup> CCSD(T)/6-311++G(2d,2p) results from ref 27 in parentheses. <sup>c</sup> DFT(B3LYP)/6-311++G(3df,3pd) results from ref 28 in parentheses.

SCF, and QCISD methods. We showed that the triplet state exhibits a 33 kcal/mol energy barrier as determined at the CAS SCF level. DFT methods located this barrier at a shorter C-N bond distance with a 12 kcal/mol lower energy than does CAS SCF. In this work, Table 1 reports the optimized equilibrium structures of these states at a more exhaustive level of theory for the purpose of discussion and completeness.

There have been numerous theoretical and experimental studies of the ground state of nitromethane,<sup>27-29</sup> nitramine,<sup>30-32</sup> and nitric acid,<sup>33-36</sup> all of which reported C<sub>s</sub> symmetry and X-NO<sub>2</sub> planar geometry. Our results in Tables 1-3 closely match these observations. CAS SCF results show shortened X-NO<sub>2</sub> bond lengths from experimental (nitramine) and perturbation-based methods of calculation (nitromethane and nitric acid). The wave functions for all species exhibit a dominant closed-shell character with some mixing of ( $\pi \rightarrow \pi^*$ ) excitation-based configurations. The optimized geometric parameters do not show any appreciable change with the use of a larger basis set.

Owing, in part, to the spin-forbidden singlet-triplet transition, experimental data on the triplet states of the nitro compounds studied in this work are lacking. The only reported work is by electron-impact spectroscopy<sup>37</sup> on nitromethane, where the lowest singlet-triplet transition was observed to have an onset at 3.1 eV and a maximum intensity at 3.8 eV. Only recently

**TABLE 2: Equilibrium Structures and Total (in hartree) and Relative Energies for the Singlet Ground State, the Triplet State, and the Singlet–Triplet Intersection of Nitramine<sup>a</sup>**

	singlet <sup>b</sup>	triplet	singlet–triplet MECP
<i>R</i> (N–H <sub>1</sub> )	0.998 (1.005) 0.996	1.002 1.000 1.014	1.000
<i>R</i> (N–H <sub>2</sub> )	0.998 0.996	1.000 0.996 1.019	1.003
<i>R</i> (N–N)	1.378 (1.427) 1.375	1.391 1.389 1.404	1.388
<i>R</i> (N–O)	1.217 (1.206) 1.206	1.323 1.317 1.301	1.364
∠H <sub>2</sub> NH <sub>1</sub>	114.5 (115.1) 114.0	109.6 109.2 109.9	110.0
∠NNH <sub>1</sub>	109.3 109.1	109.9 109.8 107.2	107.6
∠NNH <sub>1,2</sub>	122.5 121.8	118.0 117.7 118.0	120.9
∠NNO	117.4 116.8	113.8 115.1 115.8	113.0
∠ONO	126.4 (130.8) 126.5	110.3 110.2 106.8	98.2
∠ONON	177.6 177.6	133.0 132.8 134.4	116.2
<i>E</i> <sub>c</sub>	–259.793 421 –259.818 055	–259.687 126 –259.705 305 –261.031 488	–259.674 165 –259.694 295 <sup>c</sup>
Δ <i>E</i> <sup>d</sup>	–66.7 –70.8	0.0 0.0 0.0	8.1 6.9
ZPE	26.8	24.7	

<sup>a</sup> Results (top to bottom) are from CAS(6,5)/dzp, CAS SCF (6,5)/6-311++G(2d,2p), and DFT(B3LYP)/6-311++G(2d,2p) Levels of theory, respectively. Bond lengths are in angstroms, and angles are in degrees. <sup>b</sup> Experimental results from ref 29 in parentheses. <sup>c</sup> CAS SCF (6,5)/6-311++G(2d,2p) results are single-point calculations at the CAS(6,5)/dzp structure. The singlet and triplet states are degenerate to within 0.01 kcal/mol. <sup>d</sup> Energies (kcal/mol) relative to the triplet minimum.

were ab initio calculations reported on the triplet-state equilibrium structures of nitromethane<sup>24,29</sup> and nitric acid.<sup>36</sup> As reported in Tables 1–3, the triplet-state equilibrium structures for the three species differ from that of the singlet mainly in the structure of the nitro group. This group is largely bent out of plane, as can be seen in the deviation from linearity of the ONOC, ONON, and ONOO dihedral angles by approximately 50°. Recent CAS SCF calculations showed similar behavior for the triplet state of nitrobenzene.<sup>38</sup> Also, it should be noted that the N–O bond distances in all three cases have increased by 0.1 Å from the geometry of the ground state and that the ONO angle decreased by almost 15°. Examinations of the CAS SCF wave functions for the triplet states showed mixed configurations of  $\pi \rightarrow \pi^*$  and  $n \rightarrow \pi^*$  excitations of the NO<sub>2</sub> molecular orbitals. These localized excitations would explain the increase in the N–O bond distance. The CAS SCF(6,5)/6-311++G(2d,2p) calculated singlet–triplet ( $v_0 - v_0$ ) energy difference (including zero-point energy) is 61.3 kcal/mol for nitromethane,<sup>24</sup> 70.8 kcal/mol for nitramine, and 62.7 kcal/mol for nitric acid. From

**TABLE 3: Equilibrium Structures and Total (in hartree) and Relative Energies for the Singlet Ground State, the Triplet State, and the Singlet–Triplet Intersection of Nitric Acid<sup>a</sup>**

	singlet <sup>b</sup>	triplet <sup>c</sup>	singlet–triplet MECP
<i>R</i> (O–H)	0.952 (0.959) 0.947	0.951 (0.978) 0.947 0.974	0.951
<i>R</i> (O–N)	1.337 (1.406) 1.414	1.416 (1.424) 1.413 1.405	1.418
<i>R</i> (N–O)	1.207 (1.203) 1.181	1.298 (1.304) 1.289 1.291	1.324
∠NOH	104.6 (101.9) 104.5	106.4 (102.8) 106.4 105.4	106.9
∠O(H)NO	114.5 (113.9) 115.4	112.4 (110.7) 112.5 116.3	110.2
∠ONO	128.7 129.2	111.2 111.4 107.6	103.6
∠ONOO	180.0 177.8	127.0 127.4 132.5	117.8
<i>E</i> <sub>c</sub>	–279.599 651 –279.609 674	–279.490 730 –279.509 748 –280.885 503	–279.484 119 –279.504 896 <sup>d</sup>
Δ <i>E</i> <sup>e</sup>	–68.4 –62.7	0.0 0.0 0.0	4.1 3.0
ZPE	18.3	15.6	

<sup>a</sup> Results (top to bottom) are from CAS(6,5)/dzp, CAS SCF (6,5)/6-311++G(2d,2p), and DFT(B3LYP)/6-311++G(2d,2p) levels of theory, respectively. Bond lengths are in angstroms, and angles are in degrees. <sup>b</sup> Experimental results from ref 33 in parentheses. <sup>c</sup> QCISD/6-31G\* results from ref 35 in parentheses. <sup>d</sup> A single-point CAS SCF (6,5)/6-311++G(2d,2p) calculation at the CAS(6,5)/dzp structure. The singlet and triplet states are degenerate to within 0.09 kcal/mol. <sup>e</sup> Energies (kcal/mol) relative to the triplet minimum.

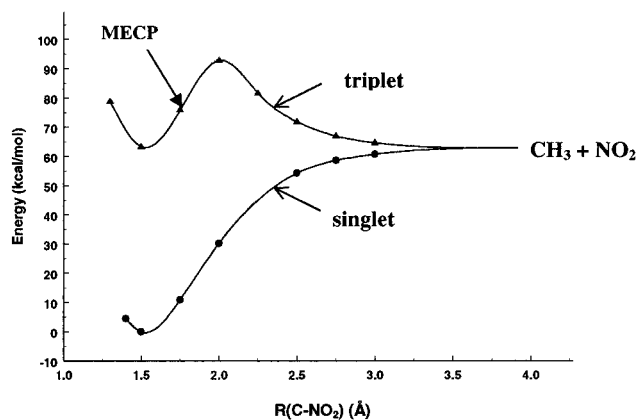
**TABLE 4: Relative Energies<sup>a</sup> of the Singlet and Triplet States of Nitromethane with Respect to the Triplet-State Minimum (in kcal/mol) from CAS SCF(6,5)/6-311++G(2d,2p) Calculations**

structure	singlet ( <i>S</i> <sub>0</sub> )	triplet ( <i>T</i> <sub>1</sub> )
CH <sub>3</sub> + NO <sub>2</sub> <sup>b</sup>	1.7	1.7
min( <i>S</i> <sub>0</sub> )	–63.2	23.6
min( <i>T</i> <sub>1</sub> )	–27.5	0.0
MECP( <i>S</i> <sub>0</sub> – <i>T</i> <sub>1</sub> ) <sup>c</sup>	16.3	14.8

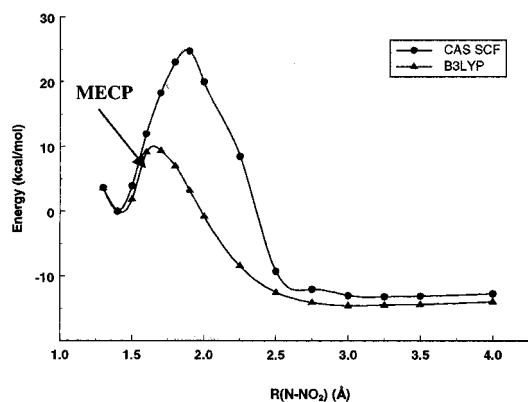
<sup>a</sup> *E* = –243.714 626. <sup>b</sup> Calculated at *R*(CN) = 8.0 Å and the experimental *R*(N–O) = 1.194 Å, ∠ONO = 133.8°, and *R*(C–H) = 1.079 Å. <sup>c</sup> Single-point calculations at the crossing structure as in Table 1.

Table 4 we note that the predicted adiabatic vertical singlet–triplet transition in nitromethane is 86.8 kcal/mol (3.8 eV), in excellent agreement with the experimental work noted above. The experimentally determined X–NO<sub>2</sub> dissociation energies are 60.1<sup>39</sup> and 49.4 kcal/mol<sup>40</sup> for nitromethane and nitric acid, respectively. For nitramine, calculated values are in the 41–48 kcal/mol range.<sup>31,32,41</sup> Thus, only the triplet of nitromethane is comparable in energy to its dissociation limit, while nitramine and nitric acid have singlet–triplet energy differences greater than the ground-state dissociation limit. We finally note that the DFT calculated parameters are in close agreement with the CAS SCF values.

To determine the adiabatic stability of the triplet state, we report fully optimized curves relative to X–NO<sub>2</sub> dissociation



**Figure 1.** CAS SCF(6,5)/6-311++G(2d,2p) fully optimized potential energy curves for the singlet and triplet states of nitromethane.



**Figure 2.** CAS SCF(6,5) and DFT(B3LYP)/6-311++G(2d,2p) fully optimized potential energy curve for the triplet state of nitramine.

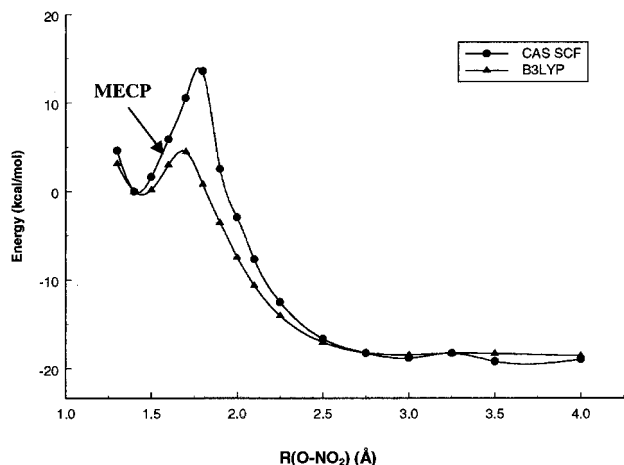


**Figure 3.** CAS SCF(6,5) and DFT(B3LYP)/6-311++G(2d,2p) fully optimized potential energy curve for the triplet state of nitric acid.

in Figures 1–3. These curves show the dependence on the X–N bond length with all other parameters optimized and do not include zero-point energy corrections. For nitromethane, the CAS SCF calculations of Figure 1 (and reported earlier<sup>24</sup>) give a 33 kcal/mol barrier. For nitramine and nitric acid, CAS SCF calculations gave 25 and 15 kcal/mol barriers, respectively. These values show that the triplet states of these molecules could support a few vibrational energy levels, rendering the state adiabatically (meta) stable. The energy curves for the triplet structures of nitramine and nitric acid shown in Figures 2 and 3 indicate that these states are metastable with respect to dissociation by 15 and 20 kcal/mol, respectively. The DFT calculations predict barriers for nitramine and nitric acid that

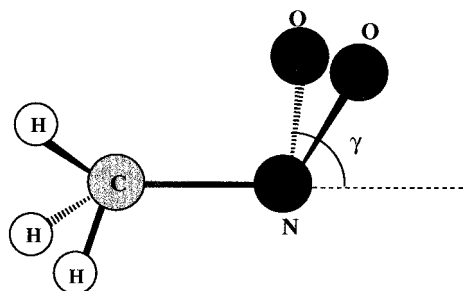


**Figure 4.** Geometric structure of nitromethane at the minimum-energy crossing point and the definition of the bending angle  $\gamma$ .

are located at shorter X–N bond lengths, with energy barriers 15 and 10 kcal/mol less than CAS SCF values, respectively. These observations are consistent with the ones reported for nitromethane.<sup>24</sup>

**2. Singlet–Triplet Minimum Energy Crossings.** The optimized geometries of the singlet–triplet minimum energy crossing points for the three molecular systems are presented in Tables 1–3. The optimized geometries exhibit mainly deformation in the  $-\text{NO}_2$  group from the corresponding triplet-state minima, as Figure 4 demonstrates in the case of nitromethane. For all three species the X–N bond length is practically unchanged, but the N–O bond distances in the  $\text{NO}_2$  group show an increase of  $\sim 0.03$ – $0.05$  Å. Most notable is a further  $\sim 15^\circ$  decrease of the ONO angle of the triplet minimum-energy structure and a  $62$ – $66^\circ$  deviation of the  $-\text{NO}_2$  from linearity. Energetically, these crossing points are 13.7, 8.1, and 4.1 kcal/mol above the triplet minima for nitromethane, nitramine, and nitric acid, respectively, as determined with the *dzp* basis. Single-point calculations with the larger 6-311++G-(2d,2p) basis changed these barriers by about 1 kcal/mol.

Examination of the geometric structures and energetics of the reported crossing points shows that they are placed very close to their corresponding triplet minima. These points establish energy barriers for the triplet state less than half of those with respect to the X– $\text{NO}_2$  adiabatic dissociation. It is expected that with typical temperatures of up to 3000 K that accompany detonation in condensed-phase explosives, these low-energy barriers could easily be overcome. To date, there has not been any experimental indication for phosphorescence-induced transitions in these systems. Therefore, the intersystem crossings reported in this work should establish nonradiative channels for the triplet-state deactivation. Recent experimental work on nitrobenzene<sup>42</sup> has shown that the triplet formation is very efficient with a quantum yield of  $\geq 80\%$ . In the same study, the lifetime of the lowest excited singlet state was reported to be very short, 10 ps, and surprisingly a short lifetime of  $\sim 480$  ps for the lowest triplet state was also detected. It was suggested that motions of the nitro group may cause the rapid relaxation from the lowest triplet state to the ground state.

Table 4 reports the energetics of the ground-state singlet and the lowest triplet states of nitromethane at various extrema, determined as CAS SCF single-point calculations with the larger basis and without state-averaging. The singlet state is 27.5 kcal/mol below at the triplet-state minimum structure. Furthermore, the singlet state undergoes a sharp energy increase ( $\sim 43$  kcal/mol) in reaching the minimum-energy crossing point, just  $\sim 14$  kcal/mol above the triplet minimum equilibrium point. Thus, motion in the  $-\text{NO}_2$  out-of-plane bending mode ( $\gamma$  in Figure 4) causes a drastic effect on the ground-state singlet surface, whereas a smooth and broad connection between the triplet minimum and the MECP for the triplet state is predicted. Figure 5 clearly demonstrates this fact, since the energies of the singlet

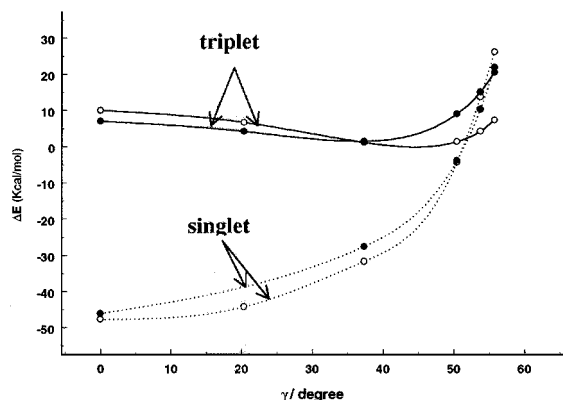


**Figure 5.** The 6-311++G(2d,2p) CAS SCF (6,5) (●) and DFT-(B3LYP) (○) energies of the triplet and singlet states of nitromethane at various bending angles relative to the triplet minimum.

and triplet states of nitromethane are calculated at various bending angles ( $\gamma$ ) of the ONO group with respect to the C–N bond. The curves were determined at a structure approximate to the optimized equilibrium structure of the triplet state, with  $R(\text{NO}) = 1.30 \text{ \AA}$  and  $R(\text{CN}) = 1.48 \text{ \AA}$ . CAS SCF calculations on nitrobenzene<sup>38</sup> showed similar behavior in which the potential curve of the triplet state along the out-of-plane  $-\text{NO}_2$  bending mode was very flat compared with that of the ground state. For nitromethane, the energy difference between the planar structure and the optimized equilibrium structure in the triplet state is only 7 kcal/mol at the CAS SCF level and 14 kcal/mol with the MECP. These energetics allow facile movement of the nitro group along large bending motions. We also calculated the Hessian matrix of the singlet state at the MECP and found that it is a saddle point with one imaginary eigenvalue ( $419 \text{ cm}^{-1}$ ) at the CAS SCF(6,5)/dzp level, a characteristic of a transition state. A reaction path calculation<sup>43,44</sup> followed the singlet state from the transition state to its equilibrium structure, which is the reaction coordinate consisting mostly of the nitro group bending. From the difference in curvature for the triplet and singlet states along this bending mode, one expects a large Franck–Condon factor contribution for the triplet–singlet intersystem crossing, as noted previously.<sup>42,45</sup> Along with the spin–orbit coupling, the efficiency of the intersystem transition is also influenced by the energy difference gradient of the two states in the vicinity of the MECP.

On the basis of the above, it is expected that thermal activation in nitromethane along the nitro bending mode permits efficient, nonradiative energy transfer from the triplet state to higher vibrational levels of the ground-state singlet. Recently,<sup>46</sup> experimental work established a very short nonradiative lifetime of about 1 ps for the excited singlet state of nitromethane. The results further showed that 76% of the energy deposited in the sample was released nonradiatively. Juxtaposed with our results, vibrationally hot ground-state molecules could thus be generated by fast internal conversion and intersystem crossing. If electronic excitation plays a role under high pressure and temperature events such as those in the initiation process of energetic materials, these de-excitation mechanisms should be taken into account for a molecular level description of decomposition channels.

#### IV. Conclusion

We report ab initio CAS SCF calculations locating the minimum energy on the lowest singlet–triplet intersection surface in model energetic compounds: nitromethane, nitramine, and nitric acid. Triplet curves fully optimized with respect to

the X–NO<sub>2</sub> dissociation channels gave adiabatic energy barriers of 33, 25, and 15 kcal/mol for these materials, respectively. The triplet states of the molecules considered exhibit equilibrium structures in which the NO<sub>2</sub> group is no longer coplanar with carbon, in striking contrast to the singlet structures. Singlet–triplet minimum-energy crossing points were located at 13, 8, and 4 kcal/mol above the respective triplet equilibrium geometries. For nitromethane, it is shown that the nitro group bending potential energy curve of the triplet state has a broad and almost flat structure, in contrast to the singlet curve. The intersystem crossings could allow for fast nonradiative energy transfer from the excited triplet to the ground states, thus speeding up the vibrational excitation process occurring in the gas-phase under shock compression. Future work will consider the effect of compression on the energetics of electronic excitation, interstate conversion, and intersystem crossings. Studies along the line of the current work have been initiated for energetic materials of interest such as TATB and RDX.

**Acknowledgment.** This work was performed under the auspices of the U.S. Department of Energy by the Lawrence Livermore National Laboratory under Contract W-7405-Eng-48. The authors thank Professor L. J. Butler and Dr. C. M. Tarver for useful comments about the manuscript.

#### References and Notes

- (1) Michl, J.; Bonacic-Koutecky, V. *Electronic Aspects of Organic Photochemistry*; Wiley: New York, 1990.
- (2) Koga, N.; Morokuma, K. *Chem. Phys. Lett.* **1985**, *119*, 371.
- (3) Yarkony, D. R. *J. Chem. Phys.* **1990**, *92*, 2457.
- (4) Farazdel, A.; Dupuis, M. *J. Comput. Chem.* **1991**, *12*, 276–282.
- (5) Bearpark, M. J.; Robb, M. A.; Schlegel, H. B. *Chem. Phys. Lett.* **1994**, *223*, 269.
- (6) Agrawal, J. P. *Prog. Energy. Combust. Sci.* **1998**, *24*, 1.
- (7) Engelke, R.; Sheffield, S. A. *Initiation and Propagation of Detonation in Condensed-Phase High Explosives*; Davison, L., Shahinpoor, M., Eds.; Springer-Verlag: New York, 1998; Vol. III.
- (8) Blais, N. C.; Engelke, R.; Sheffield, S. A. *J. Phys. Chem. A* **1997**, *101*, 8285.
- (9) Winey, J. M.; Gupta, Y. M. *J. Phys. Chem. B* **1997**, *101*, 10733.
- (10) Wang, J.; Brower, K. R.; Naud, D. L. *J. Org. Chem.* **1997**, *62*, 9048.
- (11) Gruzdkov, Y. A.; Gupta, Y. M. *J. Phys. Chem. A* **1998**, *102*, 2322.
- (12) Tokmakoff, A.; Fayer, M. D.; Dlott, D. D. *J. Phys. Chem.* **1993**, *97*, 1901.
- (13) Tarver, C. M. *J. Phys. Chem. A* **1997**, *101*, 4845.
- (14) Fried, L. E.; Ruggerio, A. J. *J. Phys. Chem.* **1994**, *98*, 9786.
- (15) Williams, F. *Adv. Chem. Phys.* **1971**, *21*, 289.
- (16) Dremim, A. N.; Klimentov, V. Y.; Davidove, O. N.; Zoludeva, T. A. *Multiprocess detonation model: The Ninth Symposium (International) on Detonation*, Portland, Oregon; OCNR: Arlington, VA, 1989; Vol. I, p 724.
- (17) Sharma, J.; Beard, B. C.; Chaykovsky, M. *J. Phys. Chem.* **1991**, *95*, 1209.
- (18) Gilman, J. J. *Philos. Mag. B* **1995**, *71*, 1057.
- (19) Dunning, T. H.; Hay, P. J. In *Modern Theoretical Chemistry*; Schaefer, H. F., Ed.; Plenum: New York, 1976; Vol. 3.
- (20) Eade, R. H. E.; Robb, M. A. *Chem. Phys. Lett.* **1981**, *83*, 362.
- (21) Schlegel, H. B.; Robb, M. A. *Chem. Phys. Lett.* **1982**, *93*, 43.
- (22) Becke, A. D. *J. Chem. Phys.* **1993**, *98*, 5648.
- (23) Lee, C.; Yang, W.; Parr, R. G. *Phys. Rev. B* **1988**, *37*, 785.
- (24) Manaa, M. R.; Fried, L. E. *J. Phys. Chem. A* **1998**, *102*, 9884.
- (25) Frisch, M. J.; Trucks, G. W.; Schlegel, H. B.; Gill, P. M. W.; Johnson, B. G.; Robb, M. A.; Cheeseman, J. R.; Keith, T.; Petersson, G. A.; Montgomery, J. A.; Raghavachari, K.; Al-Laham, M. A.; Zakrzewski, V. G.; Ortiz, J. V.; Foresman, J. B.; Cioslowski, J.; Stefanov, B. B.; Nanayakkara, A.; Challacombe, M.; Peng, C. Y.; Ayala, P. Y.; Chen, W.; Wong, M. W.; Andres, J. L.; Replogle, E. S.; Gomperts, R.; Martin, R. L.; Fox, D. J.; Binkley, J. S.; Defrees, D. J.; Baker, J.; Stewart, J. P.; Head-Gordon, M.; Gonzales, C.; Pople, J. A. *Gaussian 94*, revision E.2; Gaussian, Inc.: Pittsburgh, PA, 1995.
- (26) Schmidt, M. W.; Baldrige, K. K.; Boatz, J. A.; Elbert, S. T.; Gordon, M. S.; Jensen, J. H.; Koseki, S.; Matsunaga, N.; Nguyen, K. A.; Su, S. J.; Windus, T. L.; Dupuis, M.; Montgomery, J. A. *J. Comput. Chem.* **1993**, *14*, 1347.

- (27) Lobo, R. F. M.; Moutinho, A. M. C.; Lacmann, K.; Los, J. *J. Chem. Phys.* **1991**, *95*, 166.
- (28) Gutsev, G. L.; Bartlett, R. J. *J. Chem. Phys.* **1996**, *105*, 8785.
- (29) Jursic, B. S. *Int. J. Quantum Chem.* **1997**, *64*, 263.
- (30) Tyler, J. K. *J. Mol. Spectrosc.* **1963**, *11*, 39.
- (31) Saxon, R. P.; Yoshimine, M. *J. Phys. Chem.* **1989**, *93*, 3130.
- (32) Roszak, S.; Kaufman, J. J. *J. Chem. Phys.* **1992**, *160*, 1.
- (33) Cox, A. P.; Riveros, J. M. *J. Chem. Phys.* **1965**, *42*, 3106.
- (34) Ghosh, P. N.; Blom, C. E.; Bauder, A. *J. Mol. Spectrosc.* **1981**, *89*, 159.
- (35) Lee, T. J.; Rice, J. E. *J. Phys. Chem.* **1992**, *96*, 650.
- (36) Grana, A. M.; Lee, T. J.; Head-Gordon, M. *J. Phys. Chem.* **1995**, *99*, 3493.
- (37) Ficker, W. M.; Mosher, O. A.; Kuppermann, A. *Chem. Phys. Lett.* **1979**, *60*, 518.
- (38) Takezaki, M.; Hirota, N.; Terazima, M.; Sato, H.; Nakajima, T.; Kato, S. *J. Phys. Chem. A* **1997**, *101*, 5190.
- (39) Pedley, J. B.; Naylor, R. D.; Kirby, S. P. *Thermochemical Data of Organic Compounds*, 2nd ed.; Chapman: New York, 1986.
- (40) Lias, S. G.; Bartmess, S. G.; Liebmann, J. F.; Holmes, J. L.; Levin, R. D.; Mallard, W. G. *J. Phys. Chem. Ref. Data* **1988**, *17*.
- (41) Melius, C. F. *Chemistry and Physics of Energetic Materials*; Butusu, S. N., Ed.; Kluwer Academic: Dordrecht, 1989.
- (42) Takezaki, M.; Hirota, N.; Terazima, M. *J. Phys. Chem. A* **1997**, *101*, 3443.
- (43) Gonzalez, C.; Schlegel, H. B. *J. Chem. Phys.* **1989**, *90*, 2154.
- (44) Gonzalez, C.; Schlegel, H. B. *J. Phys. Chem.* **1990**, *94*, 5523.
- (45) Terazima, M.; Yamauchi, S.; Hirota, N.; Kitao, O.; Nakatsuji, H. *Chem. Phys.* **1986**, *107*, 81.
- (46) Rajchenbach, C.; Jonusauskas, G.; Rulliere, C. *Chem. Phys. Lett.* **1994**, *231*, 467.